Nuclear Medicine and Biology 43 (2016) 273–279

Contents lists available at ScienceDirect

Nuclear Medicine and Biology

journal homepage: www.elsevier.com/locate/nucmedbio

[^{124}I]FIAU: Human dosimetry and infection imaging in patients with suspected prosthetic joint infection

Xiaoyan M. Zhang [a,*], Halle H. Zhang [a], Patrick McLeroth [b], Richard D. Berkowitz [c], Michael A. Mont [d], Michael G. Stabin [e], Barry A. Siegel [f], Abass Alavi [g], T. Marc Barnett [h], Jeffrey Gelb [b], Chantal Petit [b], John Spaltro [b], Steve Y. Cho [i], Martin G. Pomper [j], James J. Conklin [k], Chetan Bettegowda [l], Saurabh Saha [a,*]

[a] BioMed Valley Discoveries Inc., Kansas City, Missouri
[b] Covance, Princeton, New Jersey
[c] Phoenix Clinical Research, Tamarac, Florida
[d] The Rubin Institute for Advanced Orthopedics, Sinai Hospital, Baltimore, Maryland
[e] Department of Radiology and Radiological Sciences, Vanderbilt University, Nashville, Tennessee
[f] Mallinckrodt Institute of Radiology, Washington University School of Medicine, St. Louis, Missouri
[g] Department of Radiology, Hospital of the University of Pennsylvania, Philadelphia, Pennsylvania
[h] Mission Hospital, Ashville, North Carolina
[i] Department of Radiology, University of Wisconsin School of Medicine and Public Health, Madison, Wisconsin
[j] Russell H. Morgan Department of Radiology and Radiological Science, Johns Hopkins University, Baltimore, Maryland
[k] ICON Medical Imaging, Warrington, Pennsylvania
[l] Department of Neurology, The Johns Hopkins Medical Institutes, Baltimore, Maryland

ARTICLE INFO

Article history:
Received 29 September 2015
Received in revised form 10 December 2015
Accepted 27 January 2016

Keywords:
FIAU
PET/CT
Prosthetic joint infection
Diagnosis

ABSTRACT

Introduction: Fialuridine (FIAU) is a nucleoside analog that is a substrate for bacterial thymidine kinase (TK). Once phosphorylated by TK, [^{124}I]FIAU becomes trapped within bacteria and can be detected with positron emission tomography/computed tomography (PET/CT). [^{124}I]FIAU PET/CT has been shown to detect bacteria in patients with musculoskeletal bacterial infections. Accurate diagnosis of prosthetic joint infections (PJIs) has proven challenging because of the lack of a well-validated reference. In the current study, we assessed biodistribution and dosimetry of [^{124}I]FIAU, and investigated whether [^{124}I]FIAU PET/CT can diagnose PJIs with acceptable accuracy.
Methods: To assess biodistribution and dosimetry, six subjects with suspected hip or knee PJI and six healthy subjects underwent serial PET/CT after being dosed with 74 MBq (2 mCi) [^{124}I]FIAU intravenously (IV). Estimated radiation doses were calculated with the OLINDA/EXM software. To determine accuracy of [^{124}I]FIAU, 22 subjects with suspected hip or knee PJI were scanned at 2–6 and 24–30 h post IV injection of 185 MBq (5 mCi) [^{124}I]FIAU. Images were interpreted by a single reader blinded to clinical information. Representative cases were reviewed by 3 additional readers. The utility of [^{124}I]FIAU to detect PJIs was assessed based on the correlation of the patient's infection status with imaging results as determined by an independent adjudication board (IAB).
Results: The kidney, liver, spleen, and urinary bladder received the highest radiation doses of [^{124}I]FIAU. The effective dose was 0.16 to 0.20 mSv/MBq and doses to most organs ranged from 0.11 to 0.76 mGy/MBq. PET image quality obtained from PJI patients was confounded by metal artifacts from the prostheses and pronounced FIAU uptake in muscle. Consequently, a correlation with infection status and imaging results could not be established.
Conclusions: [^{124}I]FIAU was well-tolerated in healthy volunteers and subjects with suspected PJI, and had acceptable dosimetry. However, the utility of [^{124}I]FIAU for the clinical detection of PJIs is limited by poor image quality and low specificity.

1. Introduction

A major challenge in the treatment of prosthetic joint infection (PJI) is the difficulty in distinguishing infection from sterile inflammation. Often, there is uncertainty regarding whether a prosthetic joint is infected or simply loose. Multiple factors currently considered by clinicians attempting to make a diagnosis include medical history; physical

* Corresponding authors at: BioMed Valley Discoveries Inc., 4520 Main Street, Suite 1650, Kansas City, MO 64111. Tel.: +1 781 533-9412.
E-mail addresses: mzhang@biomed-valley.com (X.M. Zhang), ssaha@biomed-valley.com (S. Saha).

http://dx.doi.org/10.1016/j.nucmedbio.2016.01.004

examination findings; imaging findings on radiographs, computed tomography (CT) and bone scintigraphy; pre-operative laboratory evaluations (leukocyte count and differential, erythrocyte sedimentation rates [ESR], C-reactive protein [CRP], leukocyte esterase); and the findings from pre-operative joint aspirates [1,2]. Sometimes, the infection only can be ascertained intra-operatively through histology and culture of specimens [3]. There is seldom any single pre-operative test that is definitive [4,5], because current diagnostic tests have suboptimal sensitivity and specificity [6]. Even after surgery, there are cases where the level of diagnostic certainty is low, especially for infections caused by indolent organisms or those with fastidious growth requirements [7,8]. A misdiagnosis has important consequences. If infection is missed, prosthesis revision without appropriate débridement and antibiotic treatment, risks early failure and infection recrudescence. Conversely, a false-positive diagnosis of prosthetic infection may result in unnecessary invasive procedures, such as single or multi-staged revisions [9,10].

Various radiopharmaceuticals have been investigated as potential imaging agents to diagnose PJI, but all have important limitations [11–14]. Bone scintigraphy measuring dynamic uptake of bone-seeking tracers such as ^{99m}Tc-labeled diphosphonates, is used extensively to assist the clinical management of numerous osseous pathologies and is characterized by high sensitivity but low specificity for diagnosis of PJI. At the present time, bone scintigraphy is used primarily for screening purposes to exclude the possibility of any kind of loosening of the prosthesis. In vitro radiolabeled leukocyte scintigraphy has been extensively studied for diagnosis of prosthesis infection but has also yielded variable and often contradictory results. This has been attributed to differences in acquisition, analysis, and interpretation protocols between investigators and in patient characteristics impacting sensitivity (presence of biofilm around the infected prosthesis and influence of antibiotics) or specificity (non-specific inflammation and interference from ectopic bone marrow) [12]. Enhanced techniques (late leukocyte scintigraphy, dual or serial time point leukocyte scintigraphy, in vivo labeled leukocyte scintigraphy) and combination modalities with bone scintigraphy, bone marrow scintigraphy, SPECT or SPECT/CT have been developed, some with important improvement on the accuracy of infection diagnosis [13]. However, the complex labeling procedures, the need to handle hazardous blood products, and cost remain disadvantages for labeled leukocyte-based modalities [11,14]. Other techniques such as [^{18}F]fluorodeoxyglucose ([^{18}F]FDG) PET and scintigraphy with the radiolabeled antibiotic ^{99m}Tc-ciprofloxacin (Infecton) have also been studied but neither is able to consistently differentiate infection from aseptic inflammation. The published results on the role of FDG PET in diagnosing PJI are controversial, reflecting the challenges in image interpretation criteria, generation of artifacts, uptake by activated macrophages around inflamed prostheses, and the nonspecific uptake by healing tissues post arthroplasty surgery [12,13]. The discrepancy in the reported Infecton performance was probably due to biofilm, low bacteria count or resistance, and different labeling kit formulations [12]. Therefore, radiopharmaceuticals that can reliably differentiate infection from aseptic inflammation yet can be prepared routinely with commercially available materials are warranted.

Preclinical data from a mouse model of infection demonstrated that localized infections could be readily imaged with ^{125}I-FIAU, a nucleoside analog that is a substrate for bacterial thymidine kinase (TK) and labels bacteria at infection sites [15]. Subsequently, positron emission tomography (PET) with [^{124}I]FIAU was evaluated in a small human study of eight patients with suspected musculoskeletal infections and one control subject [16]. The [^{124}I]FIAU findings of infection versus non-infection in all eight patients were consistent with those made based on preoperative and intraoperative assessments, including cultures. The preclinical and limited clinical data suggest that [^{124}I]FIAU might be a promising agent for diagnosing infections, including PJIs.

This prospective study assessed the dosimetry and safety of [^{124}I]FIAU in humans and the utility of [^{124}I]FIAU PET/CT in diagnosing PJIs.

2. Materials and methods

This study was conducted in two parts. Part I, a phase 1 trial (http://clinicaltrials.gov, NCT01337466) in two centers (Supplemental Table S1), evaluated biodistribution and dosimetry of [^{124}I]FIAU by PET/CT in patients with hip or knee PJI and healthy subjects. Part II, a phase 2 trial (http://clinicaltrials.gov, NCT01705496) in 8 centers (Supplemental Table S1), evaluated the sensitivity and specificity of [^{124}I]FIAU PET/CT in patients presenting with pain in a prosthetic knee or hip. All procedures performed in studies involving human participants were in accordance with the ethical standards of the institutional and/or national research committee and with the 1964 Helsinki declaration and its later amendments or comparable ethical standards.

2.1. Patients and Eligibility Criteria

Both trials were approved by the respective institutional review boards at the participating sites. Prior to enrollment, all subjects gave written informed consent.

Subjects with suspected PJI were required to have a prosthetic joint implant in situ for >3 months prior to enrollment and were required to have operative intervention planned within 30 days following study enrollment. Women were either postmenopausal or surgically sterile. Subjects with a history of an inherited mitochondrial disorder, abnormal liver function, or hypersensitivity to iodine were excluded. No subjects, except for one, received antibiotics in the 2 weeks preceding imaging.

For thyroid protection, either saturated solution of potassium iodide (SSKI) or Lugol's iodine was administered 1 h prior to dosing and continued for 7 days. Alternatively, potassium iodide tablets were administered beginning 1 day prior to dosing and continued for 8 days.

A total of 12 subjects (6 healthy and 6 with suspected PJI) were enrolled in the phase 1 study and each received a single dose of 70.67–86.58 MBq (1.91–2.34 mCi) [^{124}I]FIAU (except for 1 subject receiving 45.88 MBq because of a calibration error). The subjects underwent whole-body PET/CT immediately after injection. Imaging was repeated at 2, 4, and 6 h after dosing for all subjects; additional imaging at 24, 48, and 72 h after dosing was required for healthy subjects and optional for subjects with suspected PJI. A low-dose CT protocol, performed at 120 kVp and with mA as low as reasonably achievable, was used for attenuation correction. The effective dose for each CT scan at the two phase 1 sites was approximately 1.5–2 mSv. The PET data from 10 subjects were used for estimation of dosimetry; images for the other 2 subjects were excluded from the dosimetry analysis because of image acquisition and/or decay-correction errors.

For the phase 2 trial, 22 subjects with suspected PJI received a single dose of 159.5–210.9 MBq (4.3–5.7 mCi) [^{124}I]FIAU and 19 completed the study. Two subjects discontinued early as “lost to follow-up”, and one subject withdrew from the study. PET/CT of the area of interest (hip or knee) was performed twice, 2–6 and 24–30 h, respectively, after dosing.

Safety was assessed by adverse event and vital sign monitoring, clinical laboratory tests (serum chemistry including liver function tests, complete blood count, and CRP), and physical examination for up to 30 days after dosing. All 34 subjects from both phase 1 and 2 were included in the safety analysis.

2.2. Radiopharmaceutical

Each dose of [^{124}I]FIAU [[^{124}I]1-(2-deoxy-2-fluoro-β-D-arabinofuranosyl)-5-iodo-(2,4(1 H,3 H)-pyrimidinedione] was produced individually by 3D Imaging LLC. The specific activity was characterized as 999–1295 GBq (27–35 Ci)/μmole (carrier-free), with >90% radiochemical purity (remainder sodium iodide), and >99% radionuclidic purity (remainder I-125). The administered mass of FIAU was up to 0.12 μg.

[^{124}I]FIAU was supplied and shipped as a ready-to-inject sterile isotonic saline solution with 5% ethyl alcohol as anti-radiolytic agent and 50 mM of sodium phosphate as buffering agent, pH 5.5–8.5 with a shelf life of one half-life of ^{124}I (4.2 days from synthesis time).

2.3. Image Analysis

Attenuation-corrected PET images were reconstructed with an iterative reconstruction based on scanner manufacturer's recommendations. The 3–5 mm thick transaxial CT images were reconstructed at contiguous intervals (or manufacturer's recommendation for overlap) for fusion with the transaxial PET images. CT, attenuation-corrected (AC) PET, metallic artifact algorithm attenuation-corrected PET (if available), and non-attenuation-corrected (NAC) PET images were generated and submitted to Icon Medical Imaging (IMI) for central archiving and data analysis using a proprietary Medical Image Review and Analysis (MIRA™) system.

PET image review was conducted using dedicated PET software from MIM Software. The collected data were presented to a single reader (JJC), blinded to clinical information, in sequential order, for a qualitative assessment of both AC and NAC PET images. Target-to-background ratios using the suspected infected joint as the target and the contralateral muscle mass as the background, and standardized uptake values (SUVmax, SUVmean and SUVpeak) were assessed. Representative cases were then presented to 3 additional readers (BAS, AA, SYC) for further evaluation.

2.4. Biodistribution and Dosimetry

Radioactivity concentrations were determined in various organs by extraction of count data from PET images using MIPAV software [17]. Activity in each visualized organ and the total body were expressed as fractions of injected activity, normalizing the activity in the whole body at the earliest time point to 100% of the administered activity. Values of the fraction of injected activity per organ were fit using SAAM II software [18]. Time-activity integrals [19] were entered into OLINDA/EXM software [20], using the adult-male model. Tracer clearance was assumed to only occur via urinary excretion; the whole-body retention curve was used to establish the kinetics of urinary excretion. Calculations were made for assumed 3.5, 2.0 and 1.0 h bladder voiding intervals. Theoretical calculations were also performed, assuming complete renal obstruction in the subjects (all kidney and total body activity assumed to be removed only by radioactive decay).

2.5. Surgical Sampling

At surgery, gross findings were documented, including the presence of any purulent material or fluid, and the surgeon's impression as to whether the joint was infected. Results from microbiological and pathological studies performed as part of standard of care were recorded. In cases where the periprosthetic membrane was removed, a minimum of 6 samples from different areas and one control sample from a clinically uninfected area were obtained for histological and microbiological testing. A central pathologist assessed all samples.

2.6. Independent Adjudication Board (IAB)

The IAB consisted of three clinicians specializing in infectious diseases or orthopedics. For each case, the clinical, laboratory, microbiological, and histologic data, along with radiologic assessments of radiographs interpreted by a central radiologist, were independently reviewed by each IAB member. Agreement in infection status between at least two of the three IAB members constituted a closed case. Cases where there was not 100% concordance between the three IAB members were flagged and reanalyzed to better understand the limitations of the current diagnostic algorithm for patients with suspected PJI.

Our definition of PJI (supplemental information) is based on the modified criteria proposed by the workgroup convened by the Musculoskeletal Infection Society [1].

3. Results

3.1. Biodistribution and Dosimetry

The primary objective of the phase 1 study was to determine the biodistribution and dosimetry of [^{124}I]FIAU. Results showed that the kidney, liver, spleen, and urinary bladder received the highest radiation exposure with [^{124}I]FIAU (Fig. 1). All data were fit well with one or two exponential functions.

Radiation exposures to most organs ranged from 0.1 to 0.8 mGy/MBq, with urinary bladder wall receiving 0.32, 0.49, and 0.76 mGy/MBq with bladder voiding intervals of 1.0, 2.0, and 3.5 h after initial administration of [^{124}I]FIAU, respectively. The effective dose (ED) of [^{124}I]FIAU was approximately 0.16, 0.18, and 0.20 mSv/MBq, under the 3 assumed voiding intervals (Table 1). Accordingly, for an administered activity of 185 MBq (5 mCi), the ED ranged from 29.5 to 36.0 mSv for the three voiding intervals.

Based on model estimates, assuming complete renal obstruction (Table 1; i.e., all elimination by radioactive decay), the kidney dose approximated 6.4 mGy/MBq and the ED approximated 0.29 mSv/MBq.

Imaging optimization and image quality was improved during the conduct of the study. Photopenic areas (noted in areas of abdomen or lower torso) were eliminated and/or reduced by changing the acquisition mode from 3D to 2D on the GE DST scanner (data not shown).

3.2. [^{124}I]FIAU PET/CT Findings in Subjects With Suspected PJI

The utility of [^{124}I]FIAU PET/CT for detection of PJI was assessed by correlating scan findings determined by an independent image reviewer and the infection status assessed by the IAB. The findings were confirmed by 3 additional readers reviewing representative cases. The PET/CT interpreters relied on both AC and NAC scans for their final decision.

All [^{124}I]FIAU PET/CT images revealed strong signals around the metal prosthesis, indicating metal artifacts from CT-based attenuation correction [21]. The NAC PET images often showed dramatically reduced counts around the prosthesis, confirming that the increased PET signal around the prosthesis on AC images was most likely attributable to metal artifact, obscuring any specific but weak bacterial uptake signal. Also noted in all PET images was pronounced diffuse muscle uptake. None of the semiquantitative measures (target-to-background ratio, SUVmax, SUVmean and SUVpeak) provided a unique signature for infection that was not confounded by artifacts or muscle uptake of the tracer around the prostheses.

Among the 19 subjects with suspected PJI who completed the phase 2 study, 4 were treated as infected by the operating surgeons, although the IAB considered only 3 as infected based on the pre-defined PJI criteria. One of these three subjects (Table S2) had bilateral knee replacements, and left-sided PJI was suspected. Two of 6 samples taken from suspected areas of infection during surgery were culture positive for coagulase-negative *Staphylococcus*, and thus categorized as infected by the IAB. On the 27-h PET/CT images (Fig. 2), while metal artifacts, as indicated by bilateral posterior focal uptake (Fig. 2A), and muscle uptake (Fig. 2B) were both prominent, there was an area of greater signal in the left anterior knee by comparison with the right knee, suggesting potential bacterial uptake (Fig. 2C). Another subject (Table S3) studied at the same site and imaged with the same scanner, had a right knee replacement in 2009, but had experienced constant pain ever since. None of the pre-operative tests suggested infection. No evidence of acute inflammation or loosening was observed during surgery. Intra-operative frozen section revealed synovial tissue with chronic inflammation, granulation tissue, and reactive changes, but neither histopathology

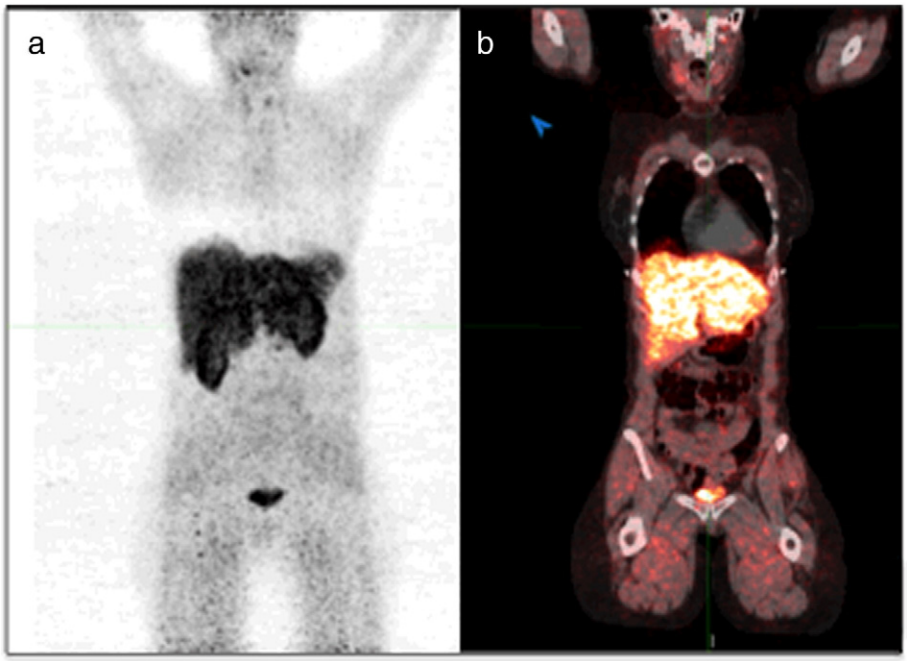

Fig. 1. Normal biodistribution of [^{124}I]FIAU. Maximal-intensity-projection (MIP) PET image (a) and fused coronal PET/CT image (b) at 4 h after injection in a healthy volunteer. Prominent activity is seen in the kidneys, liver, spleen and urinary bladder.

nor cultures of 6 surgical samples showed evidence of infection. Therefore, the joint was considered uninfected by both the surgeon and the IAB. Discordantly, intense [^{124}I]FIAU uptake was detected in the prosthetic knee and muscles (Fig. 3).

The independent PET/CT image reviewers had difficulty differentiating uninfected from infected cases based only on regional [^{124}I]FIAU uptake, primarily because of the metal artifact and high muscle background. Consequently, an independent image review charter could not be defined to guide the assessment of the PET and PET/CT images. No correlation could be established between infection status based on all clinical information and the blinded assessment of the PET/CT images.

Table 1
Average Normal Organ Dosimetry for All Subjects in Phase 1 Clinical Study.

	3.5 h void interval	2.0 h void interval	1.0 h void interval	Complete renal obstruction
	mGy/MBq	mGy/MBq	mGy/MBq	mGy/MBq
Adrenals	1.68E-01	1.68E-01	1.68E-01	4.81E-01
Brain	1.24E-01	1.24E-01	1.24E-01	1.97E-01
Breasts	1.16E-01	1.16E-01	1.16E-01	1.93E-01
Gallbladder wall	1.73E-01	1.72E-01	1.72E-01	3.76E-01
LLI wall	1.85E-01	1.77E-01	1.72E-01	2.84E-01
Small intestine	1.78E-01	1.74E-01	1.73E-01	3.34E-01
Stomach wall	1.62E-01	1.62E-01	1.62E-01	3.27E-01
ULI wall	1.73E-01	1.70E-01	1.69E-01	3.24E-01
Heart wall	1.89E-01	1.89E-01	1.89E-01	2.73E-01
Kidneys	3.08E-01	3.08E-01	3.07E-01	6.42E + 00
Liver	1.49E-01	1.49E-01	1.49E-01	2.74E-01
Lungs	1.41E-01	1.41E-01	1.41E-01	2.42E-01
Muscle	1.43E-01	1.41E-01	1.39E-01	2.51E-01
Ovaries	1.89E-01	1.81E-01	1.76E-01	2.97E-01
Pancreas	1.77E-01	1.76E-01	1.76E-01	4.19E-01
Red marrow	1.35E-01	1.34E-01	1.33E-01	2.66E-01
Osteogenic cells	2.04E-01	2.03E-01	2.03E-01	3.47E-01
Skin	1.09E-01	1.09E-01	1.08E-01	1.87E-01
Spleen	2.23E-01	2.23E-01	2.23E-01	4.57E-01
Testes	1.50E-01	1.45E-01	1.41E-01	2.21E-01
Thymus	1.46E-01	1.46E-01	1.46E-01	2.38E-01
Thyroid	1.45E-01	1.45E-01	1.45E-01	2.33E-01
Urinary bladder wall	7.57E-01	4.92E-01	3.20E-01	2.70E-01
Uterus	2.14E-01	1.95E-01	1.82E-01	2.99E-01
Total body	1.45E-01	1.43E-01	1.42E-01	2.77E-01
Effective dose (mSv/MBq)	1.95E-01	1.77E-01	1.59E-01	2.88E-01

3.3. Safety

[^{124}I]FIAU was well tolerated in healthy volunteers and subjects with suspected PJI. None of 9 adverse events (AEs) reported in the phase 1 trial was considered to be related to the study drug, none was severe, and none led to study discontinuation. Overall, 15 subjects (68.2%) from the phase 2 trial experienced AEs. However, only 2 patients, who each noted paresthesias and injection site pain, had study drug-related AEs that were mild and occurred only on the day of dosing. Only 3 AEs were severe, but none led to study discontinuation. Three subjects experienced SAEs (2 in phase 1: gastric ulcer with hemorrhage, and pain; and 1 in the phase 2: severe drug hypersensitivity to a concomitant medicine), but none of the SAEs was considered as study drug-related. No clinically meaningful trends were noted in vital signs, physical examination findings, electrocardiograms or laboratory test results, including liver function tests, lactate, serum chemistry, and complete blood count. There were no clinically detectable pharmacologic effects attributable to administration of [^{124}I]FIAU.

4. Discussion

Fialuridine (FIAU) was developed as a therapeutic agent for chronic hepatitis B infection, but the clinical program was terminated because of serious toxicity that resulted in death or the need for liver transplant among patients in a phase 2b study [22]. These serious toxicities occurred at cumulative total doses in excess of 500 mg when FIAU was administered over time with repeated dosing [23]. Importantly, the single diagnostic imaging dose of [^{124}I]FIAU used in the present study was <0.12 μg, nearly 30,000-fold lower than the lowest daily dose (~3.5 mg) administered chronically in the therapeutic studies. We have found that 74–185 MBq (2–5 mCi) [^{124}I]FIAU was well-tolerated in all subjects tested. No clinically meaningful trends were noted in the laboratory test results, including liver function tests. None of the SAEs were considered to be [^{124}I]FIAU drug related.

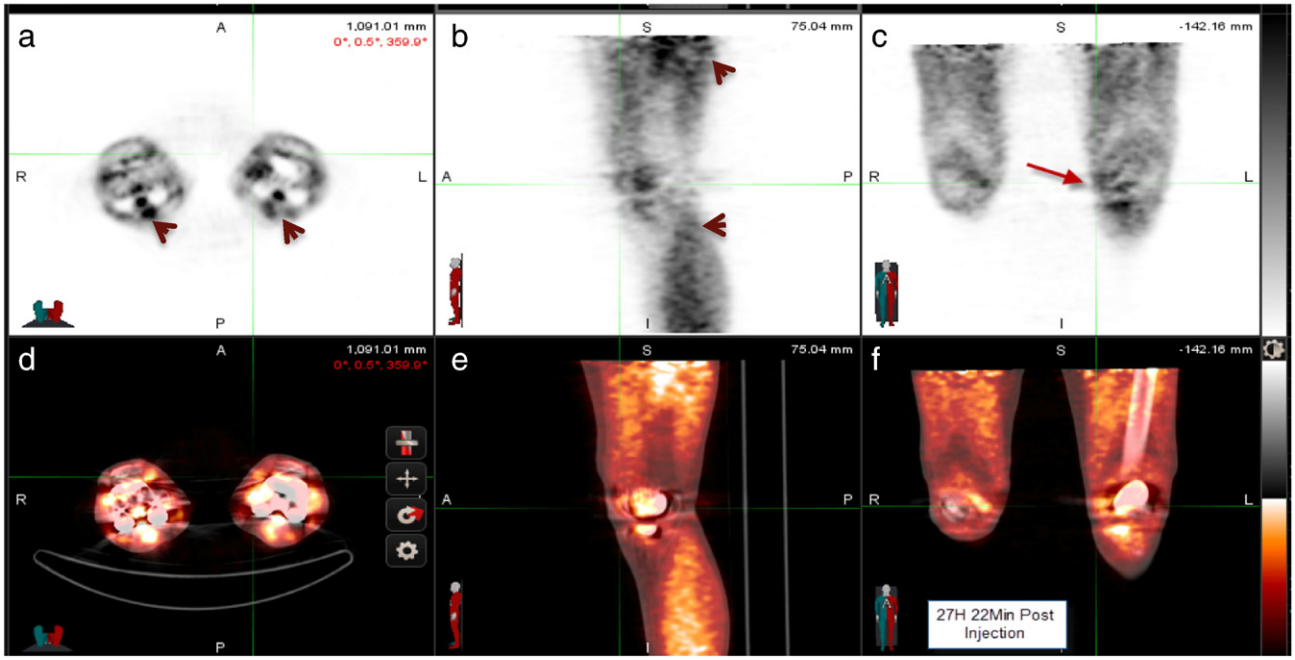

Fig. 2. True-positive scan; left knee prosthetic joint infection. The transverse, sagittal and coronal [^{124}I]FIAU PET images (a–c), and fused PET/CT images (d–f) at 27 h after injection in a patient with bilateral knee replacements show pronounced metal artifacts (arrow head, a) and muscle uptake (arrow head, b). The arrow in (c) points to the increased focal uptake in the left knee compared to the right knee.

The biodistribution of [^{124}I]FIAU is generally similar to that of radiolabeled leukocytes and [^{18}F]FDG, two other radiopharmaceuticals available for clinical diagnosis of PJI (albeit with mixed results), except for additional bone marrow uptake seen with radiolabeled leukocytes [24], and additional high brain uptake and variable myocardial and bowel uptake with [^{18}F]FDG [25]. The ED of [^{124}I]FIAU is higher for a single scan (74–185 MBq at 0.16 to 0.20 mSv/MBq), compared to that with ^{18}F-FDG (370–740 MBq at 0.019 mSv/MBq) and radiolabeled leukocytes (^{111}In-leukocytes: 10–18.5 MBq at 0.59 mSv/MBq; ^{99m}Tc-HMPAO leukocytes: 185–370 MBq at 0.017 mSv/MBq).

[^{124}I]FIAU PET/CT was evaluated for its potential utility in diagnosing PJIs. Data from a rodent model showed that bacteria-infected muscle had a much greater imaging signal than noninfected muscle [15]. In addition, a muscle infection with a *tk*-deleted *E. coli* mutant resulted in no imaging signal. These observations suggested that FIAU was effectively phosphorylated by bacterial TKs and that bacterial FIAU uptake could be readily detected by radionuclide imaging. In a small human study, Diaz et al. performed [^{124}I]FIAU PET/CT in 8 subjects with suspected musculoskeletal infections [16]. Three out of the 8 patients had suspected hip or knee PJI; [^{124}I]FIAU PET/CT was true-positive for

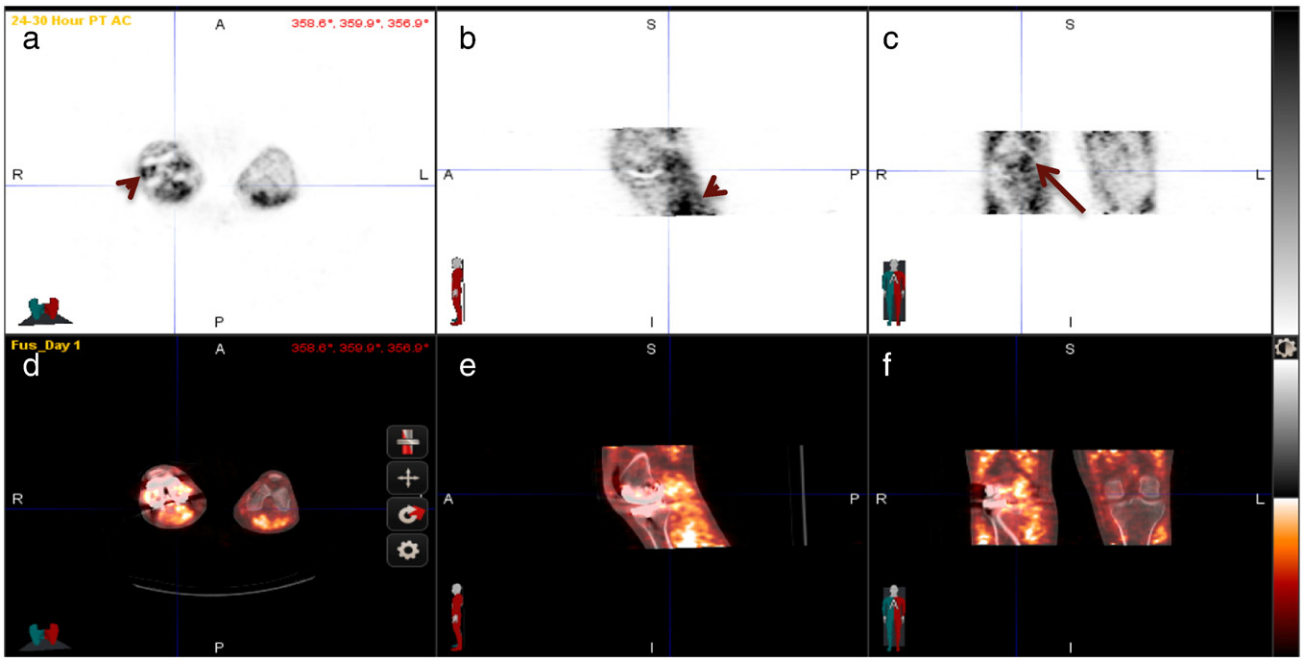

Fig. 3. False-positive scan. The transverse, sagittal and coronal [^{124}I]FIAU PET images (a–c), and fused PET/CT images (d–f) at 24 h after injection in a subject with suspected right knee PJI show pronounced metal artifacts (arrow head, a) and muscle uptake (arrow head, b). The arrow in (c) points to increased focal uptake in the right knee compared to the left knee.

infection in two, who either had positive joint aspirate culture or multiple areas of infection noted during surgery, suggesting a high bacterial load. [^{124}I]FIAU PET/CT was true negative in the third patient.

In our clinical trials, we enrolled subjects who did not have overt signs or symptoms of infection. These patients required operative intervention to correct pain in the prosthetic joint, irrespective of pre-operative test results. Because of the lack of a well-validated truth standard for diagnosing PJI, such patients pose a marked diagnostic challenge. Clinicians are often forced to explore the prosthetic joint despite no clear pre-operative diagnosis and to modify their surgery based on intraoperative findings. Many patients will have chronic and/or indolent infections with low bacterial load or subtle infections located in biofilms [26]. If the bacteria are in a quiescent state, there will be little uptake of a metabolic agent like FIAU. Further adding to the diagnostic challenges is the difficulty in detecting fastidious organisms with standard microbiological assays [7,27].

To diagnose PJI confidently in these difficult cases, an effective imaging technology must be able to detect bacterial infections with high sensitivity and specificity. Whereas, ^{18}F-FDG PET/CT imaging has been used in assessing periprosthetic infections, it cannot discriminate aseptic from septic inflammation. In our phase 1 and phase 2 PJI studies, inflammation was noted for a number of subjects in the operative reports or on histologic examination of tissue samples obtained at surgery. This observation raised the question whether the FIAU signal detected around the prosthesis of interest at least partially came from the uptake by inflammatory cells. We performed [^{124}I]FIAU PET/CT imaging in a murine collagen-induced arthritis (CIA) model to assess whether FIAU was incorporated by host inflammatory cells (supplemental information). The mouse imaging data suggest that the FIAU uptake initially increased at the inflamed sites, likely due to increased blood volume that is commonly associated with inflammation, and the uptake decreased as the agent cleared from the circulation. However, even with the 4.2-day half-life of ^{124}I, no increased [^{124}I]FIAU signal was observed in the inflamed areas of diseased animals compared to naïve animals at 24 and 48 h post-injection (Figure S1). Therefore, there was no evidence that FIAU was specifically taken up by the inflammatory cells at the joint of interest.

Nevertheless, our experience with [^{124}I]FIAU PET/CT imaging argues against its potential as a robust imaging tool for PJI diagnosis. The specificity for bacterial infection was suboptimal. Metal artifacts in CT images resulted in pronounced PET signal localized to the prosthetic joint attributable to attenuation correction artifact, making the unequivocal detection of bacteria-specific uptake very challenging, particularly in cases where only a unilateral prosthesis was present. The observed high diffuse muscle uptake of FIAU was bilateral, not limited to specific muscle groups, and involved muscles not just near the joint. There were no clearly discernable differences in muscle uptake between subjects with infected PJI and those without. The muscle uptake of [^{124}I]FIAU has also been reported by Diaz et al. in their small human study [16]. Similar findings were described in [^{18}F]FIAU studies of experimental dogs [28]. Not surprisingly, myopathy was an adverse effect associated with chronic FIAU treatment of human hepatitis B infection [23]. We hypothesize that the muscle uptake may be the result of human rather than bacterial TK activity, since FIAU is a known substrate for human TK's (cytoplasmic TK1 and mitochondrial TK2). FIAU was reported to be as good a substrate as thymidine for human TK2 [29], although the catalytic efficiency of human TK1 for FIAU was ~60 fold lower [30]. TK2 also shares more sequence similarity to bacterial TKs than TK1 does. In addition, TK1 is only expressed in S-phase cells, while TK2 is constitutively expressed in all tissues. Indeed, while TK1 is not expressed in muscle, a resting cell type, it is one of the tissues where TK2 mRNAs are predominantly expressed [31]. It is tempting to speculate that this FIAU muscle uptake reflects mitochondrial TK2 activity. Unfortunately the muscle signal markedly compromised our ability to detect bacteria-specific uptake, especially in the patients in the current study where the bacterial burden was assumed to be low. One of the major hurdles with detection of small numbers of bacteria by PET is the limited spatial resolution, which makes it extremely difficult to visualize low uptake of a targeted PET agent compared to the high surrounding background. It is also worth noting that an ^{124}I labeled tracer, with only 25.6% decay by positron emission, generally displays inferior imaging characteristics than an ^{18}F-labeled tracer, with 97% positron decay and that is typically given in much higher quantity. This has likely contributed to the low sensitivity of [^{124}I]FIAU for bacteria imaging.

The reasons for using ^{124}I-labeled instead of ^{18}F-labeled FIAU in our studies were multiple. First, chronic PJIs typically involve slow-growing bacteria. We and the study performed under RDRC approval at Johns Hopkins University (Martin Pomper and Steve Cho, personal communications) have found that delayed imaging until 24 h post FIAU dosing was required to increase specific bacterial uptake and optimize the signal-to-noise ratio in cases of infection with a low bacteria load. With an ^{18}F half-life of 109.8 min, delayed imaging at 24 h is not possible with [^{18}F]FIAU. Second, the long half-life of ^{124}I allows for once a week production in a central facility and wide distribution throughout the country to promote clinical application. Last, the synthesis of [^{18}F]FIAU is more complex and achieves much lower yield than that of [^{124}I]FIAU. We considered using [^{18}F]FIAU early on for our study, but the manufacturer could not obtain high enough yield to make this approach scalable to a level that would have been sufficient for our multi-site trials, let alone future commercial use. PET images likely would have had better resolution with [^{18}F]FIAU, but the CT streak artifacts and possibly muscle uptake would have remained problematic. Overall, compromises had to be made on the choice of tracer based on radionuclide properties, taking into account the target patient population, the long term goal of commercialization and real life logistical constraints. We could have increased the quality of the PET images by requiring scanners with metal-artifact reduction reconstruction algorithms, or scanners that can perform dual-energy CT for artifact reduction. However, since nearly all PET-CT scanners in US at the time did not have these desirable features, this would have been a limitation to wide patient access.

It is important to point out that [^{124}I]FIAU could be a potential tracer for infections caused by certain non-bacterial organisms, including Herpes-simplex virus, and other viruses with homology to HSV-1 thymidine kinase protein (HSV-1 tk), such as Epstein–Barr virus (EBV). In a clinical setting that is not confounded by metal artifacts or extremely low infection burden, FIAU may still have utility for imaging infection [32].

5. Conclusion

[^{124}I]FIAU was well-tolerated in healthy volunteers and subjects with suspected PJI, and had acceptable dosimetry. However, the utility of [^{124}I]FIAU in the detection of PJI in the clinic is limited by low image quality as a result of metal artifact and high background from non-specific muscle uptake.

Conflict of interest

Dr. McLeroth is a full time employee of Covance, a Contract Research Organization (CRO). Dr. Mont reports personal fees from DJ Orthopedics, Medical Compression Systems, Sage Products, Tissue Gene, personal fees and other from Stryker Orthopedics, outside the submitted work. Dr. Mont is an editor for the Journal of Bone and Joint Surgery, the Journal of Arthroplasty, the American Journal of Orthopedics, the Journal of Knee Surgery, Surgical Techniques International, and an editor for Orthopedics. Dr. Stabin received personal fee from Covance. Dr. Siegel received support from BioMed Valley Discoveries for the clinical trial, personal fees from GE Healthcare, Siemens Molecular Imaging, outside the submitted work. Dr. Barnett received fees from Covance for the clinical trial. Dr. Gelb was a full time employee of Covance during the conduct of study. Dr. Bettegowda has an issued

patent US111629,607. Dr. Saha has a patent methods and compositions for detecting infections pending.

Acknowledgments

We are grateful to the IAB members, Dr. Dean Tsukayama, Dr. George McKinley, Dr. Stefan Jibodh, and the central pathologist, Dr. Thomas Bauer, for their support of the phase 2 study.

Appendix A. Supplementary data

Supplementary data to this article can be found online at http://dx.doi.org/10.1016/j.nucmedbio.2016.01.004.

References

[1] Workgroup Convened by the Musculoskeletal Infection Society. New definition for periprosthetic joint infection. J Arthroplast 2011;26:1136–8.
[2] Zmistowski B, Della Valle C, Bauer TW, et al. Diagnosis of periprosthetic joint infection. J Orthop Res 2014;32(Suppl. 1):98–107.
[3] Sendi P, Zimmerli W. Diagnosis of periprosthetic joint infections in clinical practice. Int J Artif Organs 2012;35:913–22.
[4] Tetreault MW, Wetters NG, Moric M, Gross CE, Della Valle CJ. Is synovial C-reactive protein a useful marker for periprosthetic joint infection? Clin Orthop Relat Res 2014;472:3997–4003.
[5] Zmistowski B, Restrepo C, Huang R, Hozack WJ, Parvizi J. Periprosthetic joint infection diagnosis: a complete understanding of white blood cell count and differential. J Arthroplast 2012;27:1589–93.
[6] Del Arco A, Bertrand ML. The diagnosis of periprosthetic infection. Open Orthop J 2013;7:178–83.
[7] Choi HR, Kwon YM, Freiberg AA, Nelson SB, Malchau H. Periprosthetic joint infection with negative culture results: clinical characteristics and treatment outcome. J Arthroplast 2013;28:899–903.
[8] Janz V, Wassilew GI, Hasart O, Tohtz S, Perka C. Improvement in the detection rate of PJI in total hip arthroplasty through multiple sonicate fluid cultures. J Orthop Res 2013;31:2021–4.
[9] Parvizi J, Adeli B, Zmistowski B, Restrepo C, Greenwald AS. Management of periprosthetic joint infection: the current knowledge: AAOS exhibit selection. J Bone Joint Surg Am 2012;94, e104.
[10] Müller M, Morawietz L, Hasart O, Strube P, Perka C, Tohtz S. Diagnosis of periprosthetic infection following total hip arthroplasty– evaluation of the diagnostic values of pre- and intraoperative parameters and the associated strategy to preoperatively select patients with a high probability of joint infection. J Orthop Surg Res 2008;3:31.
[11] Palestro CJ. Nuclear medicine and the failed joint replacement: past, present, and future. World J Radiol 2014;6:446–58.
[12] Glaudemans AW, Galli F, Pacilio M, Signore A. Leukocyte and bacteria imaging in prosthetic joint infection. Eur Cell Mater 2013;25:61–77.
[13] Gemmel F, Van den Wyngaert H, Love C, Welling MM, Gemmel P, Palestro CJ. Prosthetic joint infections: radionuclide state-of-the-art imaging. Eur J Nucl Med Mol Imaging 2012;39:892–909.
[14] van der Bruggen W, Bleeker-Rovers CP, Boerman OC, Gotthardt M, Oyen WJ. PET and SPECT in osteomyelitis and prosthetic bone and joint infections: a systematic review. Semin Nucl Med 2010;40:3–15.
[15] Bettegowda C, Foss C, Cheong I, et al. Imaging bacterial infections with radiolabeled 1-(2′-deoxy-2-fluoro-o -D-arabinofuranosyl)-5-iodouracil. Proc Natl Acad Sci U S A 2005;102:1145–50.
[16] Diaz L, Foss C, Thornton K, et al. Imaging of musculoskeletal bacterial infections by [^{124}I]FIAU-PET/CT. PLoS One 2007;2, e1007.
[17] McAuliffe MJ, Lalonde FM, McGarry D, et al. Medical image processing, analysis and visualization in clinical research. IEEE Symposium on Computer-Based Medical Systems (CBMS); 2001. p. 381–6.
[18] Foster DM. Developing and testing integrated multicompartment models to describe a single-input multiple-output study using the SAAM II software system. Adv Exp Med Biol 1998;445:59–78.
[19] Stabin MG, Siegel JA. Physical models and dose factors for use in internal dose assessment. Health Phys 2003;85:294–310.
[20] Stabin MG, Sparks RB, Crowe E. OLINDA/EXM: the second-generation personal computer software for internal dose assessment in nuclear medicine. J Nucl Med 2005;46:1023–7.
[21] Roth TD, Maertz NA, Parr JA, Buckwalter KA, Choplin RH. CT of the hip prosthesis: appearance of components, fixation, and complications. Radiographics 2012;32:1089–107.
[22] McKenzie R, Fried M, Sallie R, et al. Hepatic failure and lactic acidosis due to fialuridine (FIAU), an investigational nucleoside analogue for chronic hepatitis B. N Engl J Med 1995;333:1099–105.
[23] Institute of Medicine (US) Committee to Review the Fialuridine (FIAU/FIAC) Clinical Trials. In: FJ Manning, Swartz M, editors. Review of the fialuridine (FIAU) clinical trials. Washington, DC: National Academies Press (US); 1995.
[24] Datz FL. The radiation dosimetry and normal value study of ^{99m}Tc-HMPAO-labeled leukocytes. Investig Radiol 1994;29:443–7.
[25] Jones SC, Alavi A, Christman D, Montanez I, Wolf AP, Reivich M. The radiation dosimetry of 2 [F-18]fluoro-2-deoxy-D-glucose in man. J Nucl Med 1982;23:613–7.
[26] Arnold WV, Shirtliff ME, Stoodley P. Bacterial biofilms and periprosthetic infections. Instr Course Lect 2014;63:385–91.
[27] Parvizi J, Erkocak OF, Della Valle CJ. Culture-negative periprosthetic joint infection. J Bone Joint Surg Am 2014;96:430–6.
[28] Nimmagadda S, Mangner TJ, Douglas KA, Muzik O, Shields AF. Biodistribution, PET, and radiation dosimetry estimates of HSV-tk gene expression imaging agent 1-(2'-deoxy-2'-^{18}F-fluoro-beta-D-arabinofuranosyl)-5-iodouracil in normal dogs. J Nucl Med 2007;48:655–60.
[29] Wang L, Munch-Petersen B, Herrström Sjöberg A, Hellman U, Bergman T, Jörnvall H, et al. Human thymidine kinase 2: molecular cloning and characterisation of the enzyme activity with antiviral and cytostatic nucleoside substrates. FEBS Lett 1999;443:170–4.
[30] Wang J, Eriksson S. Phosphorylation of the anti-hepatitis B nucleoside analog 1-(2'-deoxy-2'-fluoro-1-beta-D-arabinofuranosyl)-5-iodouracil (FIAU) by human cytosolic and mitochondrial thymidine kinase and implications for cytotoxicity. Antimicrob Agents Chemother 1996;40:1555–7.
[31] Johansson M, Karlsson A. Cloning of the cDNA and chromosome localization of the gene for human thymidine kinase 2. J Biol Chem 1997;272(13):8454–8.
[32] Fu DX, Tanhehco YC, Chen J, et al. Virus-associated tumor imaging by induction of viral gene expression. Clin Cancer Res 2007;13:1453–8.